

Characteristics of drifting subpulses

ANDRZEJ SZARY^{1,2}

and

JOERI VAN LEEUWEN^{1,3}

ASTRON

physical conditions at the polar cap

1) ASTRON, the Netherlands Institute for Radio Astronomy, 2) Janusz Gil Institute of Astronomy, University of Zielona Góra,
3) Anton Pannekoek Institute for Astronomy, University of Amsterdam

Single pulses

Single pulses of many pulsars appear to drift across the main pulse window at a fixed rate. We can characterize this drifting behaviour using the characteristic spacing between subpulses, P_2 , and the period at which a pattern of pulses repeats, P_3 (see Fig. 1).

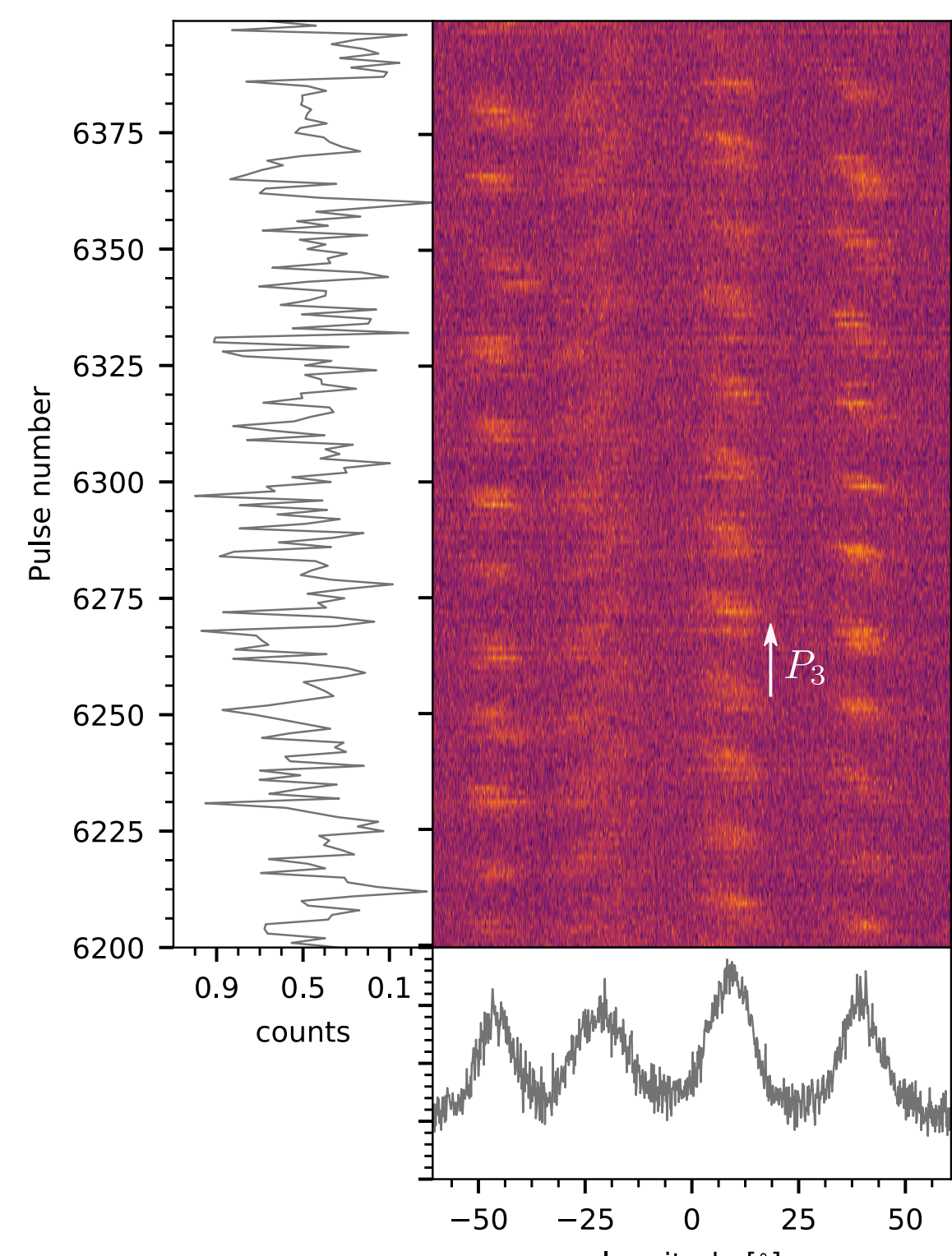


Fig. 1) Single pulses in PSR J0815+0939.

The LRFS

To quantify drifting behaviour we employed the longitude resolved fluctuation spectra (LRFS) which involves discrete Fourier transforms of consecutive pulses along each longitude. A Fourier transform produces complex numbers, which can be separated into two parts. The absolute value for a given frequency represents the amount of that frequency in the signal (see the left panel in Fig. 2), while the complex component allows to study the subpulse motion throughout the pulse window (see the top panel in Fig. 2).

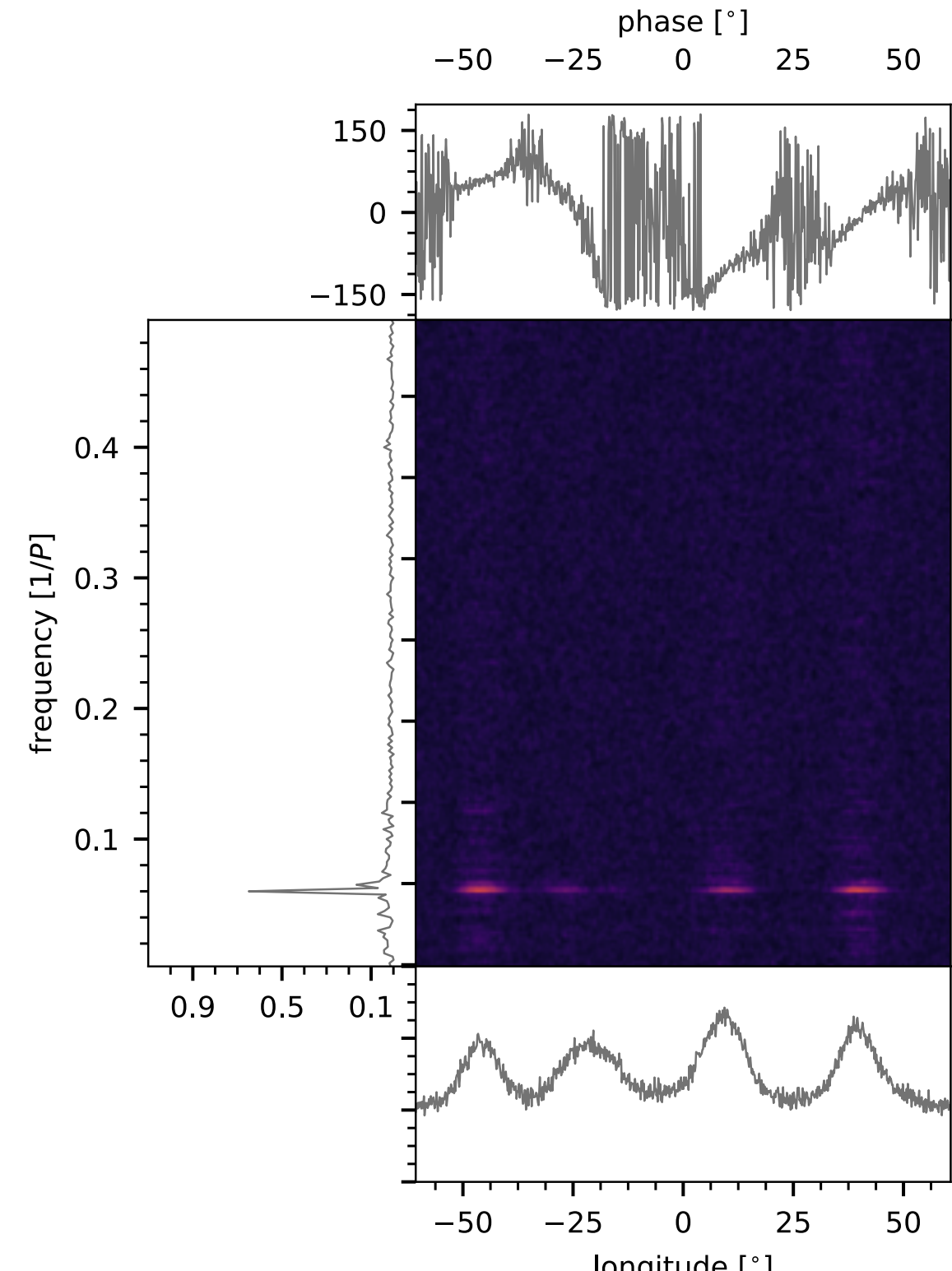


Fig. 2) LRFS plot for the single-pulse signal presented in Fig. 1.

P_3 - folded profile

The Fourier analysis results in $P_3 = 16.62 \pm 0.31 P$. We used this value to create the folded profile of the sequence of single pulses in PSR J0815+0939 (see Fig. 3). We have shown for the first time that the first component in J0815+0939 exhibits subpulse drift in the same direction, toward earlier arrival, as components III and IV, making the diametrically opposite motion of component II even more striking (see also the top panel in Fig. 2).

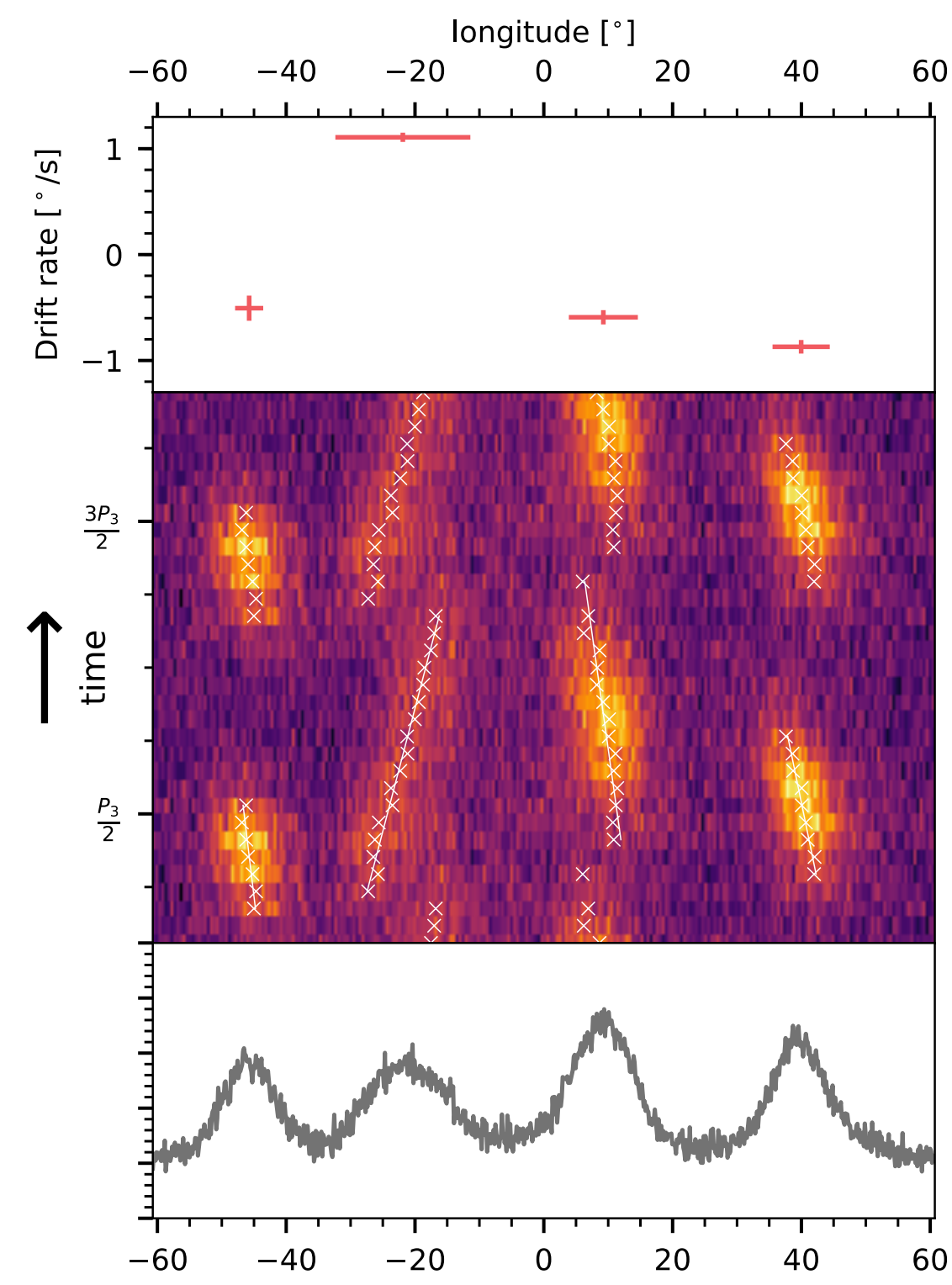


Fig. 3) Average driftband profile, obtained by folding the single-pulse signal with $P_3 = 16.62 P$.

Theoretical background

The physics governing the plasma generation in the polar cap region is a major remaining piece of the pulsar puzzle that is not completely solved. In our studies, we adopt the general approach of Ruderman & Sutherland (1975), where sparks form in regions of local maxima of the electrical potential. The electric field between the sparks is influenced by the charge deficiency in the spark-forming regions. We have found that a random distribution of sparks across the polar cap leads to drift of plasma around the global potential maximum at the polar cap (see Fig. 4). Thus, the variation of the polar-cap electric potential in the co-rotating frame, V' , can be used to determine the drift direction:

$$v' = \frac{c(\tilde{\mathbf{E}}_{\perp} \times \mathbf{B})}{B^2}, \quad (1)$$

where $\tilde{\mathbf{E}}_{\perp} = -"nabla"V'$ is the electric field perpendicular to the magnetic field in the co-rotating frame (see Szary & van Leeuwen (2017) for more details).

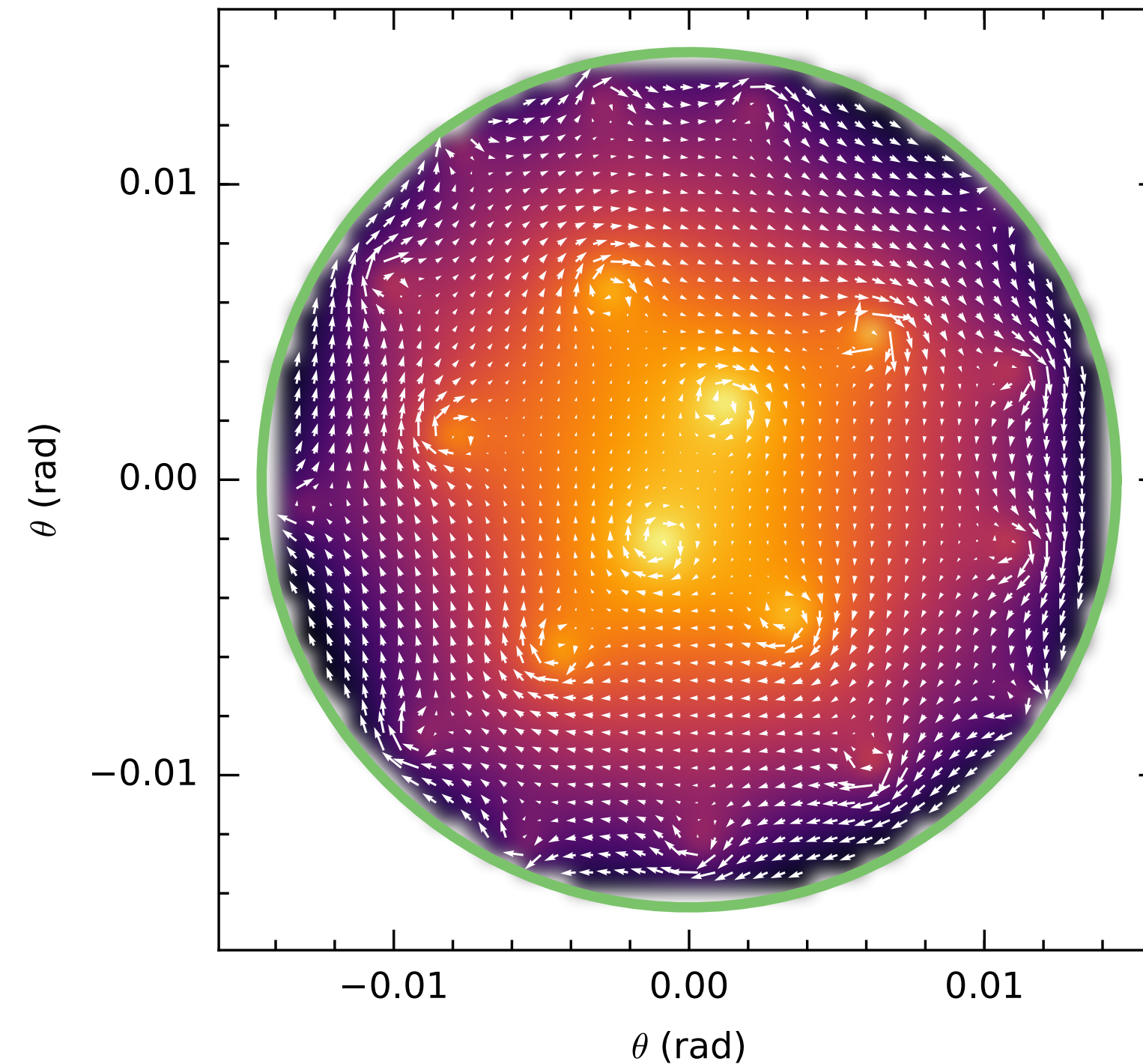


Fig. 4) Plasma velocity (the white arrows) across the polar cap for a random distribution of sparks. The color map corresponds to the electric potential.

The model

The plasma responsible for radio emission is generated and accelerated in the inner acceleration region (IAR) just above the polar cap, while the radio emission is generated at much higher altitudes. Thus, to model the observed drift characteristics we track plasma just above the polar cap region and check how this behaviour translates to the radio emission zone (~ 500 km). We model the magnetic field using prescription presented in Gil et al. 2002.

The modelling procedure is as follows:

- neutron star setup (pulsar geometry, magnetic field configuration)
- calculation of open magnetic field lines and lines connected to the line of sight (see Fig. 5a)
- electric potential setup (see Fig. 5b)
- calculation of drift direction at the polar cap (see Fig. 5b) and in the emission zone (see Fig. 5c)

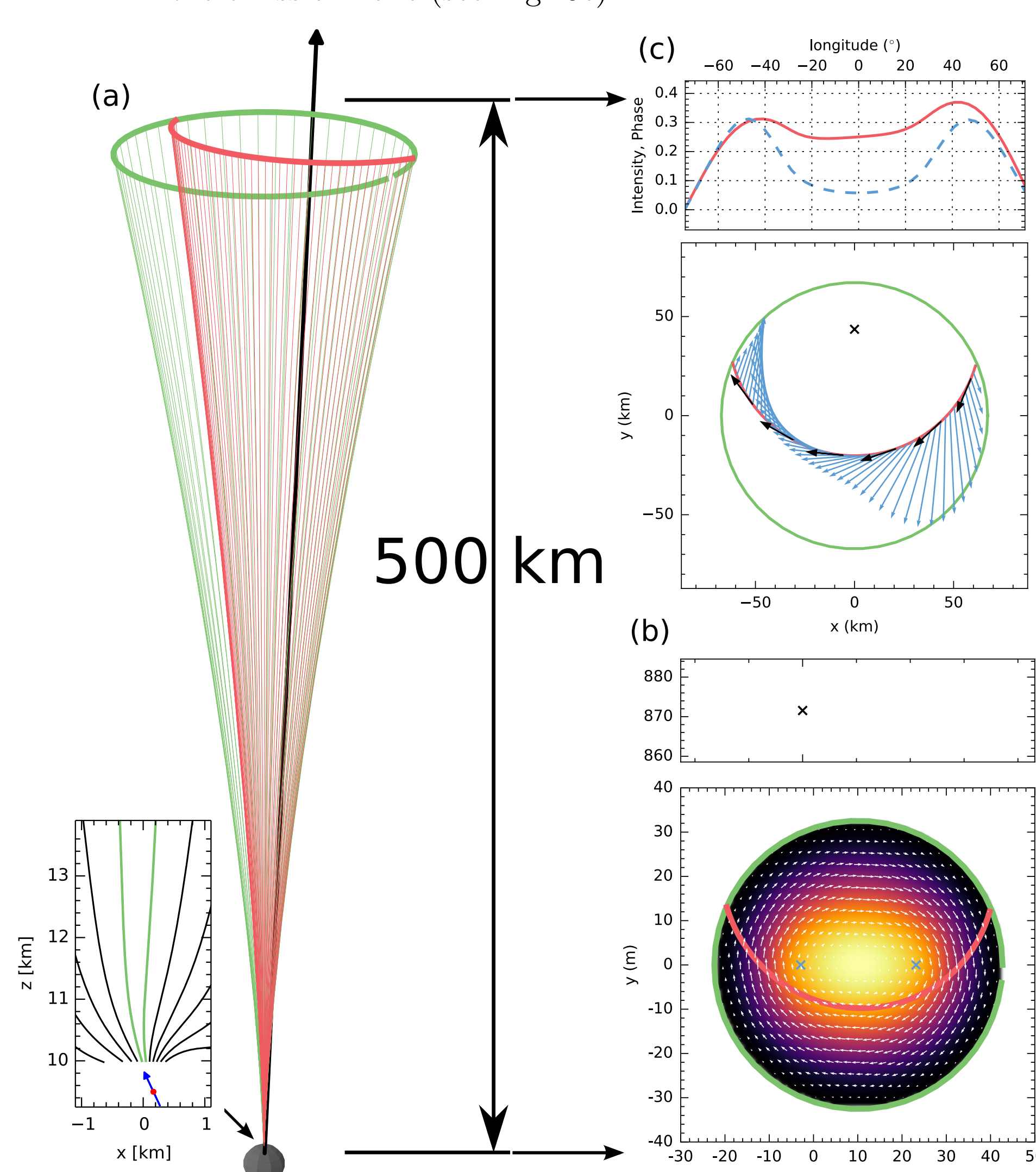


Fig. 5) Magnetic field configuration (a), electric potential setup (b), and the drift characteristics (c).

Simulations

To reproduce the bi-drifting phenomenon in J0815+0939 we calculated the drift characteristics for 10^5 realizations with purely dipolar configuration of magnetic field (with random positions and amplitudes of electric potential maxima), and 10^5 realizations with non-dipolar surface magnetic field. We showed that the bi-drifting behavior can only be explained using a non-dipolar configuration of the surface magnetic field (see Fig. 6).

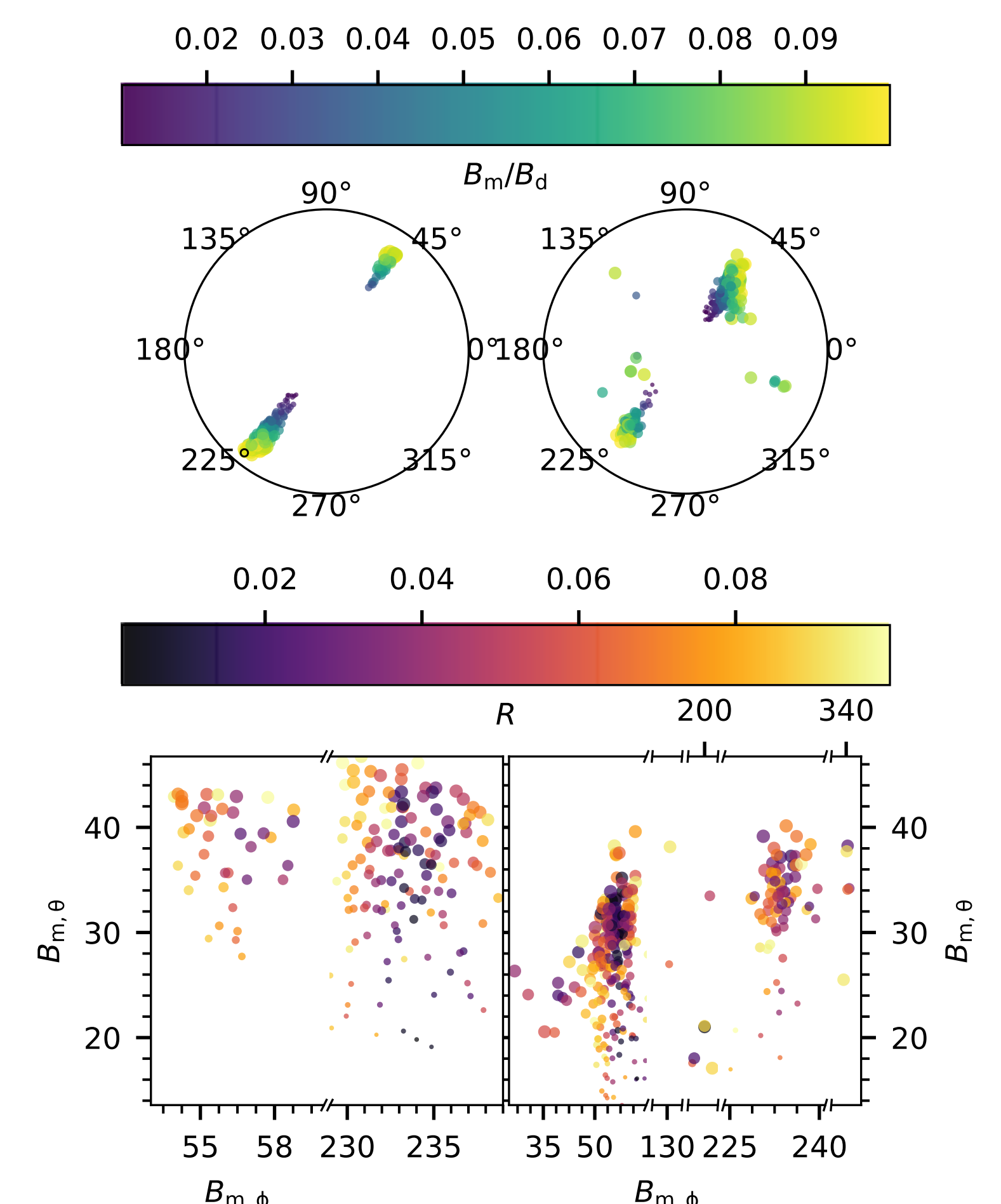


Fig. 6) Locations of magnetic anomalies for realizations showing bi-drifting behaviour. The left panels correspond to the low-field cases, while the right panels correspond to the high-field cases.

Polar cap conditions

The surface magnetic field strength falls into one of two regions of acceptable solutions, with either a relatively low ($\sim 10^{12}$ G), or high ($\sim 10^{14}$ G) surface magnetic field (see Fig. 7). Statistically, the strong-field solutions are more likely, as we find that 0.3% realizations show bi-drifting behavior (compared to 0.175% with low-field realizations). It is worth mentioning that the strong surface magnetic field is consistent with predictions of the partially screened gap model. We found that depending on the strength of the surface magnetic field, the radius of the curvature of magnetic field lines ranges from 10^5 to 10^7 cm.

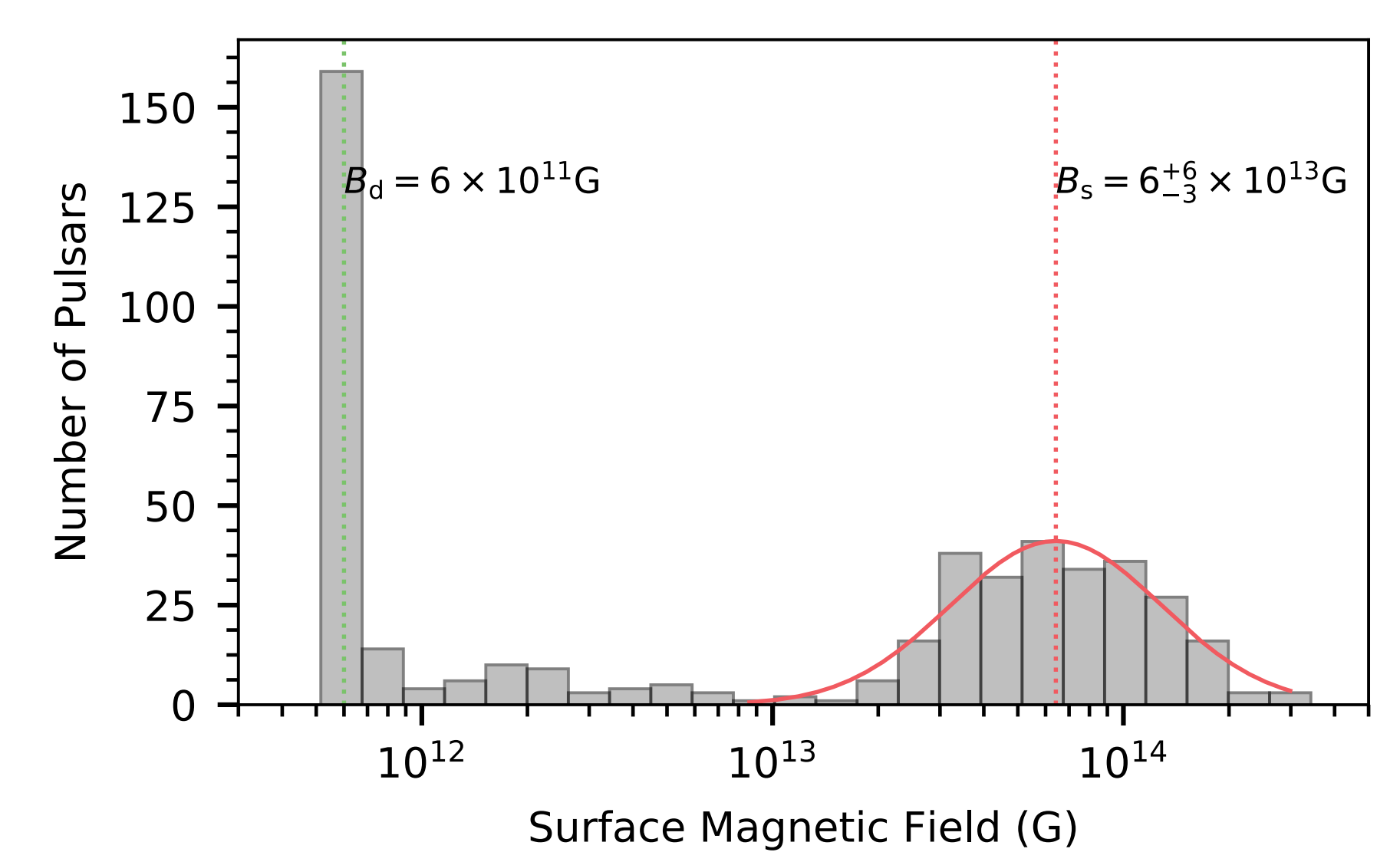


Fig. 7) Surface magnetic field for realizations showing the bi-drifting behavior.

Summary

Using a physically justified model we were able to explain the extraordinary drift properties of PSR J0815+0939. We connected radio emission properties to the conditions in the IAR, and see this as a harbinger of hope for better understanding of pulsar plasma generation processes.

References

- Gil, J. A., Melikidze, G. I., & Mitra, D. 2002, A&A, 388, 235
Ruderman, M. A., & Sutherland, P. G. 1975, ApJ, 196, 51
Szary, A., & van Leeuwen, J. 2017, ApJ, 845, 95

Contact info

e-mail: szary@astron.nl

facebook: [andrzej.szary.uz](https://www.facebook.com/andrzej.szary.uz)

